Evaluation of Satellite-Derived Latent Heat Fluxes

JÖRG SCHULZ

Max-Planck-Institut für Meteorologie, Hamburg, Germany

JENS MEYWERK AND STEFAN EWALD

Meteorologisches Institut, Universität Hamburg, Hamburg, Germany

PETER SCHLÜSSEL

Colorado Center for Aerodynamics Research/University of Colorado, Boulder, Colorado

(Manuscript received 8 December 1995, in final form 16 April 1996)

ABSTRACT

A method of determining ocean–atmosphere latent heat flux using the Special Sensor Microwave/Imager (SSM/I) and the Advanced Very High Resolution Radiometer (AVHRR) is presented and evaluated. While sea surface temperatures are retrieved from AVHRR data with an accuracy of 0.5–1.0 K, the near-surface wind speed and the surface air humidity are retrieved from measurements of the SSM/I with accuracies of 1.4 m s^{-1} and 1.1 g kg^{-1}, respectively. The latent heat flux is then computed with a stability-dependent bulk parameterization model. The derived fluxes are compared to globally distributed instantaneous shipboard and buoy measurements and to monthly averages of $2° \times 2°$ longitude and latitude bins. The standard error for instantaneous flux estimates is approximately 30 W m^{-2}, and that for monthly averages decreases to 15 W m^{-2}. Additionally, a 1-yr time series of latent heat flux at the weathership M in the North Atlantic and two shorter time series during the Tropical Ocean Global Atmosphere Coupled Ocean–Atmosphere Response Experiment (TOGA COARE) and the Central Equatorial Pacific Experiment (CEPEX) in the tropical Pacific are compared to satellite measurements. The SSM/I-derived parameters, as well as the latent heat flux, are represented very well on the weathership M. During TOGA COARE and CEPEX, the near-surface humidity is sometimes systematically overestimated in the warm pool region, which results in an underestimation of the latent heat flux. Nevertheless, the representation of the latent heat flux is always in the range of the in situ measurements.

1. Introduction

Evaporation at the air–sea interface results in a transport of energy and water vapor into the atmosphere. The energy transport partly compensates losses of energy through radiation processes in the atmosphere. The global mean of this energy transport is equivalent to 26% of the incoming solar energy at the top of the atmosphere. On this account, the exchange of energy between the sea surface and the atmosphere is a major energy source for the atmospheric circulation. The exchange of water vapor and heat at the sea surface takes place simultaneously and connects the energy cycle to the hydrologic cycle. Thus, the latent heat flux causes a cooling of the upper layer of the ocean and, through the loss of water, an increase of the salinity in the oceanic mixed layer. Good estimates of latent heat flux at the sea surface (together with fluxes of momentum and sensible heat) with global coverage could be very useful for verifying coupled ocean–atmosphere models, as well as driving ocean models.

Conventionally, the latent heat flux has been estimated from bulk formulas that employ ship measurements of near-surface wind speed, air humidity, and sea surface temperature. Since the temporal and spatial resolution of ship measurements is limited, the accuracy of ship-derived fluxes is uncertain and their use in multiyear studies is doubtful (Simonot and Gautier 1989). Unlike ships, satellites offer global spatial coverage with almost consistent quality and high temporal sampling. Hence, an estimation of the three above-mentioned parameters with remote sensing techniques should lead to an improved estimation of latent heat flux and to an improved climatology.

To get an accurate estimation of the latent heat flux, it is necessary to combine information from different radiometers. The infrared spectral region is prominently suitable for estimations of the sea surface temperature. Different remote sensing techniques are described in

Corresponding author address: Dr. Jörg Schulz, Max-Planck-Institut für Meteorologie, Bundesstraβe 55, D-20146 Hamburg, Germany.
E-mail: joerg.schulz@dkrz.de

McClain (1981), Llewellyn-Jones et al. (1984), McMillin and Crosby (1984), Schlüssel et al. (1987), Walton (1988), and Barton et al. (1989). On the other hand, estimations of the near-surface wind speed are only possible in the microwave region. The first papers in this context by Wilheit et al. (1984) and Wentz et al. (1986) refer to the Scanning Multifrequency Microwave Radiometer (SMMR) onboard the *Nimbus-7* satellite. Modified algorithms for wind speed estimation based on measurements of the Special Sensor Microwave/Imager (SSM/I) are described by Goodberlet et al. (1989), Schlüssel and Luthardt (1991), and Wentz (1992).

The most difficult problem is to estimate the near-surface air humidity since current satellite soundings are not able to measure the humidity at a level of several meters above the surface. This limitation is inherent to passive remote sensing techniques used with spaceborne radiometers since the measured radiation emanates from relatively thick atmospheric layers rather than from single levels. As an approximation for monthly mean values of surface humidity Liu and Niiler (1984) and Liu (1986, 1988) have measured the atmospheric water vapor column content or the total precipitable water. This method has been applied, for example, by Eymard et al. (1989) and Simonot and Gautier (1989) to compute monthly and 10-day averages of latent heat fluxes. Simonot and Gautier (1989) have found that this method of obtaining air humidity substantially contributes to the errors in satellite-derived latent heat fluxes when computing 10-day averages. A physical explanation for this finding is the decoupling of the atmospheric boundary layer from the higher atmosphere by an increased stability in the transition layer near the top of the boundary layer (Bunker 1949). Taylor (1982) and Marchuk et al. (1990) have showed that the total precipitable water is not a good predictor for the surface humidity because the correlation between both is not high enough. Instead, they have recommended the use of the water vapor content of the atmospheric boundary layer to predict the near-surface humidity. Recently, Schulz et al. (1993) have developed a method to estimate the water vapor content of the lowermost 500 m of the atmosphere from measurements of the SSM/I. The near-surface air humidity is highly correlated to this water vapor content and can be obtained by a simple linear form. Schlüssel et al. (1995) have slightly improved this technique by directly deriving the near-surface humidity from SSM/I measurements, which results in a lower systematic error through the suppression of magnification of error propagation that occurs in the two-step method of Schulz et al. (1993).

In this paper, the above-mentioned methods are used to compute globally distributed instantaneous latent heat fluxes, as well as time series in the North Atlantic and the tropical Pacific. The datasets used for validation purposes of the method used here are described in the next section. Section 3 gives a short review of the bulk parameterization scheme used. Section 4 introduces the single parameter retrievals needed for the use in the bulk approach. The performance of the algorithm and its ability to represent time series of latent heat flux at different stations in the Tropics as well as in northern latitudes is shown in section 5. Additionally, the estimation of global monthly mean fields of latent heat flux and its quality is analyzed in the same section. The concluding section summarizes and provides an outlook for possible future improvements.

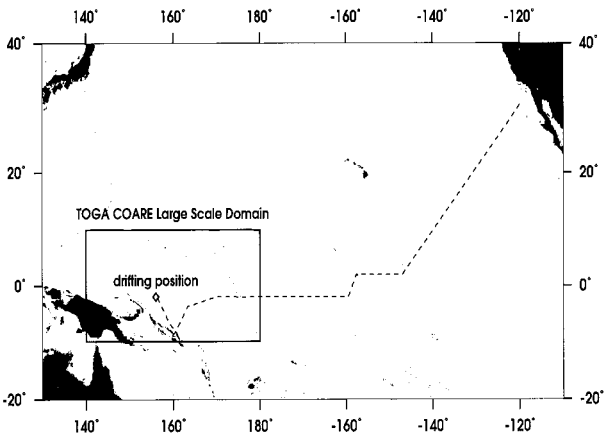

FIG. 1. Drifting position (square) and cruise (dashed line) of the R/V *Vickers* during TOGA COARE and CEPEX in February and March 1993.

2. Data

a. In situ data

To compare remotely sensed data with data measured at the sea surface, datasets provided by the National Centers for Environmental Prediction (formerly the National Meteorological Center) have been used. The data are distributed by the Scientific Computing Division of the National Center for Atmospheric Research (NCAR). For global comparisons, the period July 1987 to September 1987 has been chosen. A time series at the weathership M, which is permanently located at 66°N, 2°E is used for comparison during the period July 1987 to August 1988.

Comparisons for the tropical Pacific are undertaken with data measured during two field campaigns, named the Tropical Ocean Global Atmosphere Coupled Ocean–Atmosphere Response Experiment (TOGA COARE) and the Central Equatorial Pacific Experiment (CEPEX), that took place in the tropical Pacific. The time schedule for COARE was from November 1992 to February 1993, and CEPEX took place in March 1993. In this study, we use data from the R/V *Vickers* during February 1993, when the ship was drifting in the warm pool region near the position 2°S, 156.2°E and during CEPEX when the *Vickers* cruised at 2°S to the Christmas Islands and farther on to Los Angeles (see Fig. 1). Descriptions of these experiments can be found in the Sci-

TABLE 1. Spectral channels of used radiometers. Here, v is vertical polarization and h is horizontal polarization.

Channel	Radiometer	
	AVHRR	SSM/I
1	0.58–0.68 μm	1.55 cm (v)
2	0.725–1.1 μm	1.55 cm (h)
3	3.55–3.93 μm	1.35 cm (v)
4	10.3–11.3 μm	0.81 cm (v)
5	11.5–12.5 μm	0.81 cm (h)
6	X	0.35 cm (v)
7	X	0.35 cm (h)

entific Plan for the TOGA Coupled Ocean–Atmosphere Response Experiment (WCRP 1990) and in Dirks et al. (1992).

b. Satellite data

Only satellites provide global measurements of the required parameters, consisting of spatial averages with a nearly consistent quality and a high temporal sampling. It is well known that instruments like the Advanced Very High Resolution Radiometer (AVHRR) could be used for measurements of the sea surface temperature (T_S) under cloud-free conditions. The AVHRR measures radiation from the earth–atmosphere system in five spectral channels (see Table 1). All five channels are located in spectral regions with a high transmission of the cloud-free atmosphere. In the cloud-free case, the radiation is from the earth surface; otherwise, it is from the upper layers of clouds. The horizontal resolution of the measurements is 1.1 km at nadir and 5.6 km at the full viewing angle of 55.4°. This results in a swath width of almost 3000 km that is large enough to cover the earth surface within 1 day, giving sea surface temperatures over large portions of the World Ocean. A complete coverage is achieved within 1 or 2 weeks, depending on the actual cloud coverage.

While the sea surface temperature is measured in the infrared spectral region, the wind speed and the air humidity near the surface can hardly be determined in this spectral region because the emissivity of the ocean's surface at wavelengths of around 11 μm is very high and is only slightly affected by changes in the wind-induced roughness of the sea surface or humidity fluctuations in the lower atmosphere. The estimation of these two parameters is successful in the microwave region, where the relative small emissivity is inversely proportional to T_S. This prevents the remote sensing of T_S with high accuracy, but it allows the estimation of wind speed and near-surface humidity.

The SSM/I that can be used to determine wind speed and near-surface humidity measures radiation at millimeter and centimeter wavelengths at vertical and horizontal polarization in seven channels (Table 1). The horizontal resolution of the SSM/I is much smaller than that of the AVHRR, with 69 $\times$ 43 km^2 at 19 Ghz and 15 $\times$ 13 km^2 at 85 Ghz. The swath width of 1394 km results in a coverage of 82% of the earth's surface within 24 h. Remaining undetected areas in the Tropics and subtropics are covered within 3 days. However, the coverage is sufficiently complete because two measurements per day are given for most areas of the globe.

In this study, SSM/I data from the Defense Meteorological Satellite Program satellites *F8* and *F10* have been used to give estimates of latent heat fluxes for the periods of comparison mentioned above. The satellites were launched in July 1987 and December 1990, respectively. More detailed information about the radiometers can be found in Lauritson et al. (1979) for the AVHRR and in Hollinger (1987) for the SSM/I.

It should be mentioned here that for flux computations during TOGA COARE and CEPEX not enough cloud-free AVHRR pixels have been found, due to the persistent cloud cover in that area. Instead, bulk sea surface temperatures measured aboard the *Vickers* were used. As a consequence, the error achieved during these periods reflects only errors in the near-surface wind speed and the near-surface air humidity.

3. Bulk parameterization

The energy exchange at the air–sea interface caused by evaporation and condensation can be described by

$$E = \overline{\rho} l \overline{w'q'} \cong -\overline{\rho} l K_e \frac{\partial \overline{q}}{\partial z}, \tag{1}$$

where E is the latent heat flux density, or flux for short; ρ is the air density; l is the latent heat of evaporation; w is the vertical component of velocity; q is the specific humidity near the surface; K_e is the turbulent diffusion coefficient; and z is the height. Horizontal bars indicate a 10-min time average, and primes indicate an actual deviation from the time average.

Measuring methods such as the profile method and the cross-correlation method that are able to determine E with (1) and the so-called dissipation method, which is based on an assumed relation between E and the spectra of surface wind speed and near-surface humidity (Smith 1988), have the main disadvantage that they require a large expenditure of work. Thus, they are not suitable to determine E routinely.

Usually, the bulk method is used to estimate latent heat fluxes from rudimentary shipboard measurements. The bulk formula parameterizes the flux mainly as a function of near-surface wind speed, air humidity, and sea surface temperature. Hence, the flux is given by

$$E = -\overline{\rho} l C_E \overline{u}(\overline{q} - \overline{q}_S), \tag{2}$$

where u is the surface wind speed, q_S is the specific saturation humidity at the sea surface temperature T_S, and C_E is the Dalton number. If u, q, and q_S could be retrieved from satellite measurements, the bulk formula might be suitable to estimate latent heat fluxes from satellite-measured quantities (Liu 1988; Simonot and

Gautier 1989). In addition to the measured quantities, some assumptions regarding the surface pressure and the near-surface air temperature are needed to determine the air density, latent heat of evaporation, and the Dalton number. The surface pressure is assumed to be at a constant value of 1013.25 hPa. Errors due to the unawareness of surface pressure are on the order of 1% and could be neglected since the errors in the bulk formula tend to compensate each other. An overestimation of the surface pressure leads to an underestimation of q_S, but to an overestimation of ρ. To determine the air temperature, slightly unstable conditions were assumed (Wells and King-Hele 1990) and the air temperature was taken as sea surface temperature $T_S - 1$ K. The consequence of this assumption for the error contributions to the derived flux of ρ and l is not very strong since it leads to relative errors of only about 2%.

The Dalton number is computed following a parameterization given by Smith (1988). Since C_E is a function of wind speed and atmospheric stability (Liu et al. 1979), the assumption of a constant air–sea temperature difference can have a relative large effect on the estimated flux if stable conditions at low wind speeds (e.g., $\Delta T = 5$ K and $u = 5$ m s^{-1}) occur instead of the assumed slightly unstable conditions. Then, the right Dalton number would be only half as large as the used one. At highly unstable conditions (e.g., $\Delta T = 20$ K) such as during a cold air outbreak, the error in C_E is on the order of 10% at moderate wind speeds (e.g., 10 m s^{-1}). At high wind speed, the dependence of C_E on the air–sea temperature difference almost vanishes and the error in C_E goes down to 2%. The above-described cases do not occur very often, so we can conclude on the whole that the error in C_E might be on the order of a few percent. Other sources of air temperature such as model-based analyses might be superior to the above assumption, but then the latent heat flux could not be determined from satellite measurements alone.

During TOGA COARE, a modified version of the Liu et al. (1979) flux algorithm that was especially adjusted for the conditions in the tropical ocean areas has been used. A comparison of latent heat fluxes computed with this new algorithm and that of Smith (1988) results in slightly smaller values for the tropical areas and almost the same fluxes outside the Tropics. The new algorithm includes a parameterization scheme for an estimate of the warm layer and the cool skin of the ocean. For that parameterization, the solar irradiance and the longwave irradiance, in addition to the standard surface data as used in the Liu et al. (1979) algorithm, need to be known. A detailed description of the new bulk flux algorithm and the parameterization of the warm layer and the cool skin is given in Fairall et al. (1996b) and in Fairall et al. (1996a), respectively.

4. Remote sensing techniques

a. Sea surface temperature

One of the best known methods to estimate T_S from measurements of the AVHRR is the so called ''split-window'' method. This retrieval technique estimates T_S from the two AVHRR window channels 4 and 5 (Table 1). The split-window method is described in many papers, such as McMillin and Crosby (1984), Llewellyn-Jones et al. (1984), McClain et al. (1985), and Schlüssel et al. (1987). There are some differences in the algorithms of the different authors that are mainly caused by the way that they extract their coefficients. For example, McClain (1981) extracts the coefficients for his so-called Multi-Channel Sea Surface Temperature (MCSST) through a comparison between satellite and buoy measurements, while Schlüssel et al. (1987) obtained the coefficients through radiative transfer computations for given atmospheric and oceanic parameters and regression analysis. Thus, the MCSST algorithm is tuned to the bulk temperature because the buoy measurement is below the ocean's surface, and the method of Schlüssel et al. (1987) gives the temperature of the cool skin of the ocean. A comprehensive comparison between these two algorithms was made by Wick et al. (1992). They found a mean difference of 0.47 K, which is only partly caused by the difference between bulk and skin temperature. Another reason for differences between the algorithms is the dependence on the viewing angle of the radiometer that is neglected in the McClain algorithm. The advantage of using MCSST is that this is the temperature for which the bulk formula was designed. A disadvantage is that the effect of the cool skin is neglected. However, this might be of minor importance since the effect of the cool skin is smaller than the uncertainties in the measurements of the other parameters of the bulk formula. The standard error for the existing sea surface temperature algorithms is stated to be approximately 0.5–1.0 K.

In this study, weekly global MCSST fields, prepared by the Rosenstiel School of Marine and Atmospheric Science of the University of Miami, are used because the full AVHRR/Global Area Coverage dataset was not available to us. There are several important problems with the MCSST fields since day and night retrievals are used together. The number of day retrievals could highly be affected by detecting aerosols and clouds, while the night retrievals are much less affected (Reynolds 1993). Thus the day/night observation ratio varies considerably from location to location; some locations are primarily biased toward day and others toward night. This behavior of the MCSST algorithm plays an important role in the comparison with weathership M data, as discussed in section 5.

b. Wind speed

For the estimation of the near-surface wind speed from SSM/I measurements, an algorithm published by Schlüssel (1995) is used. This algorithm is a modified version of that proposed by Schlüssel and Luthardt (1991). It derives the wind speed mainly from the brightness temperature difference between horizontally and

vertically polarized components at the same frequency. The accuracy for the globally valid passive wind speed retrieval is 1.4 m s^{-1} under conditions where no heavy rain hampers the surface-leaving radiation in reaching the satellite. In cases when light rain occurs, the accuracy decreases to approximately 1.6 m s^{-1} (Schlüssel 1995).

The retrieval was evaluated by Schlüssel and Luthardt (1991) by a comparison of satellite-derived wind speeds with objectively analyzed in situ wind speeds over the North Sea (Luthardt 1985) during the period July 1987 to June 1988. They obtained a standard error of 1.9 m s^{-1}, with a small bias of 0.2 m s^{-1}. Another comparison was carried out by Schulz (1993). He compared 3403 globally distributed buoy and ship measurements with retrieved wind speeds during the period July 1987 to September 1987 and found a standard error of 2.1 m s^{-1}, with the same bias as over the North Sea. The systematic error is only significant at wind speeds above 15 m s^{-1} and could be caused by an insufficient parameterization of the emissivity of the ocean's surface. However, this is difficult to prove since there are only a few measurements during high wind speeds and, moreover, still fewer measurements of the emissivity in the microwave region under these conditions. The algorithms of Goodberlet et al. (1989) and Wentz (1989) were applied as well during the same period, but the performance is almost the same.

c. Air humidity

Using a retrievable vertically integrated water vapor content as a predictor is a common way to determine the near-surface air humidity q from satellite measurements. A useful estimation of q without temporal averaging requires a very close relationship between both quantities. This close relationship is not given for the total precipitable water W used by Liu (1986), as shown by Schlüssel (1989). He has investigated the correlation between adjacent atmospheric layers and atmospheric layers separated by a distance of 50 hPa or more. The vertical profiles of the correlation show values larger than 0.9 for adjacent layers and values larger than 0.8 for layers with a distance of 50 hPa. However, the correlation profile always shows a significant minimum near the mean height of the atmospheric boundary layer whenever the distance between the layers is larger than 50 hPa. This indicates a decoupling of the moisture in the boundary layer from that in the higher atmosphere. A similar study was done by Liu (1990); he showed vertical profiles of the variance of semidaily and daily radiosonde ascents for two tropical stations and one station in the midlatitudes. All three variance profiles show a maximum at approximately 800 hPa that indicates a high variability of the water vapor above the atmospheric boundary layer. Variance profiles of monthly mean values show this maximum only very weakly, and that is the reason why Liu and Niiler (1984) found a polynomial relation between monthly averages of q and W.

To get a good estimate of q from SSM/I measurements without temporal averaging, Schulz et al. (1993) developed a retrieval for the integrated water vapor content w_l of the lowermost 500 m of the atmosphere. From a set of globally distributed radiosonde ascents, which is representative of the variability of the earth's marine atmosphere and ocean parameters, they found a correlation of 0.98 between q and w_l.

From a sensitivity study with a radiative transfer model, Schulz et al. (1993) extracted information about those SSM/I channels that are suitable for a retrieval of w_l. It is not possible to obtain w_l from a single channel approach since all channels are influenced strongly by more than one quantity. Variations of wind speed, for example, make the horizontally polarized brightness temperatures useless as main predictors for w_l, but they are necessary for a correction of this effect. Radiative transfer computation and a multivariate regression analysis based on the above-mentioned set of radiosonde ascents results in

$$w_l = a_0 + a_1T_1 + a_2T_2 + a_3T_3 + a_4T_4, \qquad (3)$$

where $a_0 = -5.9339$ (g cm^{-2}), $a_1 = 0.03697$ (g cm^{-2} K^{-1}), $a_2 = -0.0239$ (g cm^{-2} K^{-1}), $a_3 = 0.01559$ (g cm^{-2} K^{-1}), $a_4 = -0.00497$ (g cm^{-2} K^{-1}), and T_i is the brightness temperature of channel i (see Table 1). The estimated standard error for the retrieval scheme (3) is 0.06 g cm^{-2}. The developed method is capable of resolving low-level water vapor with an accuracy that accounts for short-term fluctuations typical of observations over oceanic areas, at least for humid boundary layers. The relation between q and w_l is linear, so that q can easily be determined from

$$q = -0.53 + 19.49w_l, \qquad (4)$$

where w_l is entered in g cm^{-2} and q is retrieved in g kg^{-1}, with an accuracy of 1.2 g kg^{-1}.

The accuracy of the w_l retrieval has been confirmed by a comparison of the satellite derived w_l with w_l's is computed from radiosonde ascents, which were distributed over all ocean areas during the period from 9 July 1987 to 24 August 1987. A slightly higher standard deviation (0.09 g cm^{-2}) with no bias was found, which is caused by the time and location difference of the matched measurements, as well as by errors of the radiosonde measurements and errors due to the retrieval model itself. This standard error has been confirmed by a similar comparison done by Chou et al. (1995) for February and August 1988.

Schlüssel et al. (1995) have slightly improved this retrieval by using a direct approach of q from SSM/I measurements that avoids the error propagation that occurs in the two-step method. The retrieval reads

$$q = b_0 + b_1T_1 - b_2T_2 + b_3T_3 - b_4T_4 - b_5T_5, \qquad (5)$$

where $b_0 = -80.23$ (g kg^{-1}), $b_1 = 0.6295$ (g kg^{-1} K^{-1}),

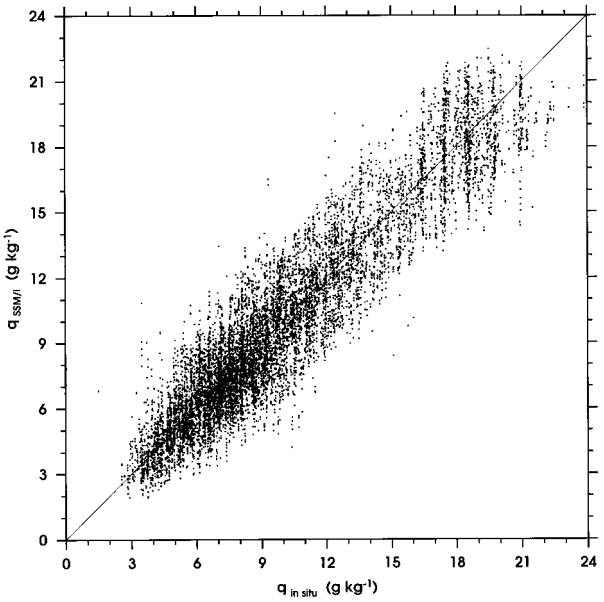

FIG. 2. Comparison between the near-surface humidity derived from SSM/I measurements and merchant ship measurements.

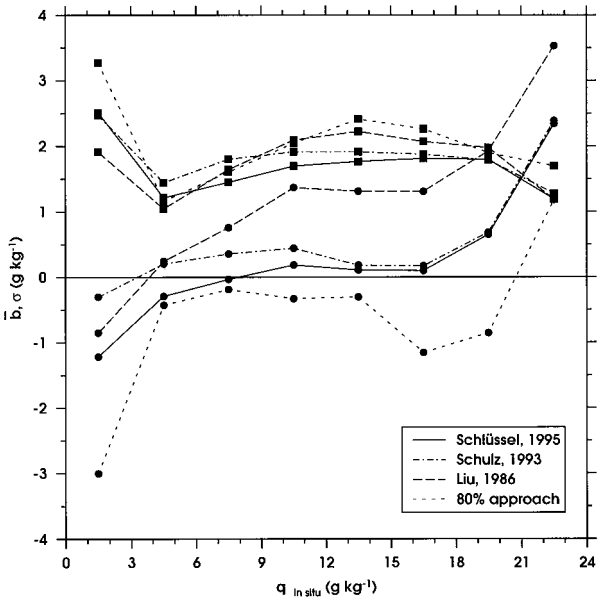

FIG. 3. Bias $\bar{b}$ and standard deviation σ from in situ measurements for four different methods. Curves for systematic errors are marked with circles, and curves for standard deviations are marked with squares. Solid lines refer to the method of Schlüssel et al. (1995), dashed–dotted lines to the method of Schulz et al. (1993), long dashed lines to the method of Liu (1986), and short dashed lines to the 80% approach, respectively.

$b_2 = 0.1655$ (g kg^{-1} K^{-1}), $b_3 = 0.1495$ (g kg^{-1} K^{-1}), $b_4 = 0.1553$ (g kg^{-1} K^{-1}), $b_5 = 0.06695$ (g kg^{-1} K^{-1}), and T_i is the brightness temperature of channel i (see Table 1). The estimated standard error for the retrieval scheme (5) is 1.1 g kg^{-1}.

To validate this retrieval with globally distributed oceanic surface measurements, some comparison criteria are necessary. The SSM/I measurements must be within a distance of 50 km from the location of the surface measurement, and they must match the surface measurements within a time window of 1 h. These criteria could be met simultaneously by more than one SSM/I measurement, and such measurements are highly correlated with each other. Nevertheless, we use all match-ups to maximize the sample. Additionally, all SSM/I measurements contaminated with heavy rain are rejected by a rain flag system after Goodberlet et al. (1989).

The comparison criteria are met in 11108 cases, and as seen in Fig. 2, there is a good agreement between ship observations and SSM/I measurements of q. At the upper end, the retrieved values of q are systematically lower than the in situ values. The reason for this could be the restriction of q during the retrieval development to values of $1 \leq q \leq 22$ g kg^{-1}. Now, higher values of q appear in the in situ dataset, which cannot be perfectly reproduced by the retrieval. However, the statistical result is dominated by specific humidities in the range $3 \leq q \leq 15$ g kg^{-1}. The bias is 0.06 g kg^{-1}, which is negligible, and the standard deviation is 1.6 g kg^{-1}. The larger error compared to the theoretical error is mostly caused by the time and location differences of the measurements.

If Liu's (1986) polynomial of the fifth order is applied to individual SSM/I-derived total precipitable water content W, the errors in q are much higher. Figure 3 shows a comparison between three methods of deriving q (Liu 1986; Schulz et al. 1993; Schlüssel 1995) for the same datasets used above. In addition, q is derived by assuming the relative humidity to be 80%. The method given by Chou et al. (1995) is not incorporated since they have already shown that it gives almost the same results as the Schulz et al. (1993) method. All pairs that met the comparison criteria are classified in intervals of 3 g kg^{-1} width. For each class, the bias $\bar{b}$, defined as

$$\bar{b} = \frac{1}{N} \sum_{i=1}^{N} x_i - y_i, \tag{6}$$

and the standard deviation σ, defined as

$$\sigma = \sqrt{\frac{1}{N-1} \sum_{i=1}^{N} (b_i - \bar{b})} \tag{7}$$

with $b_i = x_i - y_i$, are computed and plotted against the in situ value of q. Obviously, all methods underestimate high values of q. One explanation is that Liu's method was developed for the monthly mean q, which never reaches such high values. Another reason is that variations in W are very small at high values of q (Liu 1986), and therefore variations in the surface humidity are not detected. The systematic underestimation of q is continued down to 10 g kg^{-1}, indicating that q could vary independently from W. The methods of Schulz et

al. (1993) and Schlüssel (1995), on the other hand, show only small systematic errors below 18 g kg^{-1}. The overall standard deviation for Liu's method is 2.0 g kg^{-1}, so that the new methods show a remarkable improvement in retrieving the near-surface air humidity. The 80% method overestimates q slightly in the middle range $6 \leq q \leq 12$ g kg^{-1} and strongly at the lower end. At the upper end, it seems to be better than the other methods, but that is a statistical artifact since the sample size is very small.

5. Latent heat flux

Before applying (2) to combine retrieved surface wind speeds, specific air humidities, and weekly mean sea surface temperatures, the weekly MCSST fields that were delivered onto a 0.18° × 0.18° grid were temporally and spatially interpolated to the SSM/I observations. Since we are combining observations on different timescales, it could be expected that an appreciable diurnal cycle in the humidity would appear exaggerated in the latent heat flux because of the temporal averaging of only one of the terms. However, the diurnal cycle of water vapor over the oceans is generally small (Jacobs 1980), and it cannot be resolved with only two SSM/I observations per day at one location because the measurement errors in W, w_l, and q are on the order of the diurnal cycle (Schlüssel 1995).

The computed fluxes were compared to fluxes parameterized from ship measurements, as described in section 3. In order to investigate the capability of reproducing the local variability of latent heat flux at a distinct location, comparisons of time series of E at the weathership M and the R/V *Vickers* during the TOGA COARE and CEPEX field campaigns were carried out. As an example, the monthly mean latent heat flux $\langle E \rangle$ for September 1987 is presented and the quality of monthly averages is evaluated through a comparison with in situ data during August and September 1987.

a. Global comparison with in situ data

The in situ data and the criteria for the comparison are the same as in section 4c, and again we have found 11 108 match-ups. As mentioned earlier, the comparison criteria could be met simultaneously by more than one SSM/I measurement for one in situ measurement. To clearly represent the result, we show in Fig. 4 only the couples with the smallest spatial distance, but the error analysis corresponds to all match-ups. The satellite-derived fluxes are slightly biased by 3 W m^{-2}, which is mostly caused by a systematic overestimation of the flux south of 40°S, where only very few in situ observations contribute to the comparison. The standard deviation of 50 W m^{-2} between $E_{\mathrm{SSM/I}}$ and $E_{\mathrm{in\ situ}}$ seems to be very high at a first glance, but it represents both errors in the satellite-derived fluxes and errors in the fluxes derived from shipboard measurements. Blanc (1987) stated that

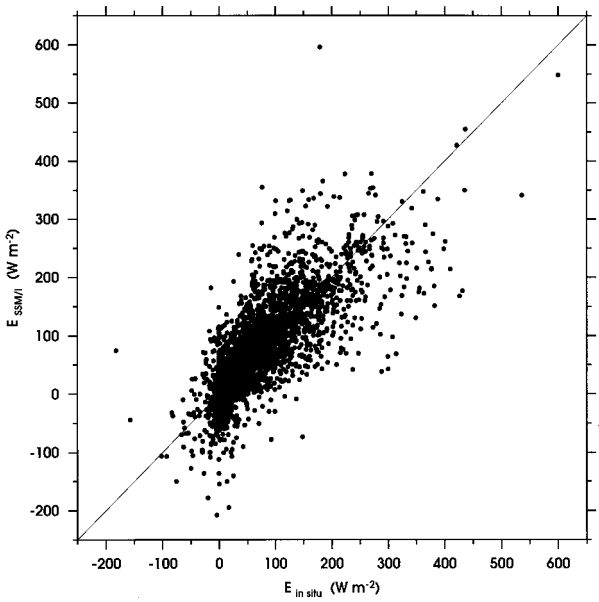

FIG. 4. Comparison between satellite-derived latent heat fluxes and latent heat fluxes parameterized from measurements of merchant ships.

the relative uncertainty of ship-derived fluxes over a range from 10 to 300 W m^{-2} is approximately 40% to 215%. These errors are estimated from a collection of well-prepared scientific experiments. In the comparison presented, mainly observations of merchant ships are used, and therefore it could be expected that the in situ flux errors are larger than that stated by Blanc (1987). However, the obtained standard deviation is smaller than that found in similar comparisons. Crewell et al. (1991) have used the total precipitable water W as a predictor for q and the scheme from Isemer and Hasse (1987) to determine C_E. They have obtained a much higher standard deviation of 73 W m^{-2} between fluxes derived from SMMR and ship measurements over the North Atlantic Ocean, although the wind speed has not been retrieved from SMMR data. In our comparison, the contribution to the standard deviation in the satellite-derived flux due to wind speed errors is 33 W m^{-2}. So it can be clearly seen that the retrieval of low-level water vapor content and the use of sea surface temperatures from AVHRR measurements considerably improve the satellite-derived fluxes.

An estimation of the absolute accuracy of satellite-derived latent heat fluxes is very difficult since the portions of the resulting standard deviation caused by in situ data or satellite data cannot be separated. However, at least 10% of the achieved standard deviation is caused by time and location differences in the measurements (Monaldo 1988). If the remaining standard deviation is distributed into equal shares for in situ and satellite-derived latent heat fluxes, then the accuracy for a single satellite observation would be 30 W m^{-2}.

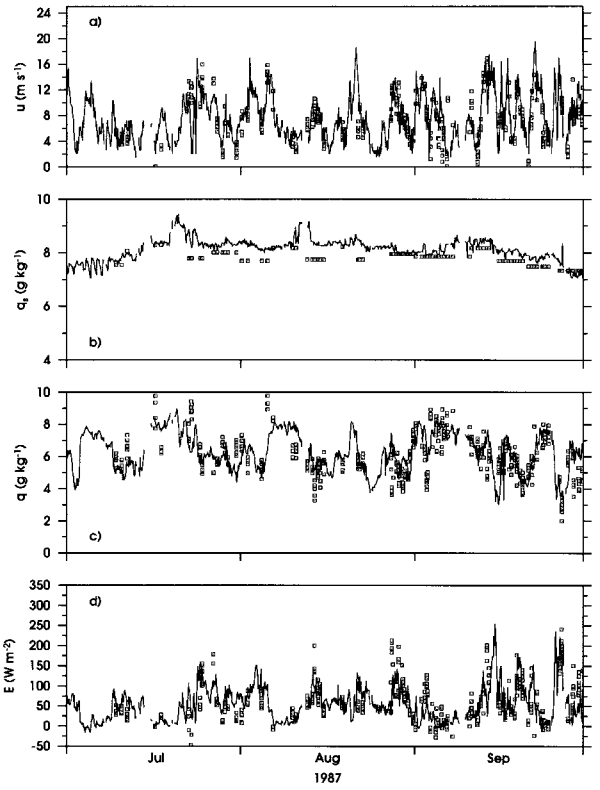

FIG. 5. Time series of (a) surface wind speed, (b) specific humidity at the sea surface temperature, (c) near-surface air humidity, and (d) latent heat flux at the weathership M in the North Atlantic during the period July 1987 to September 1987. In situ quantities are represented by solid lines, and satellite derived quantities by gray squares.

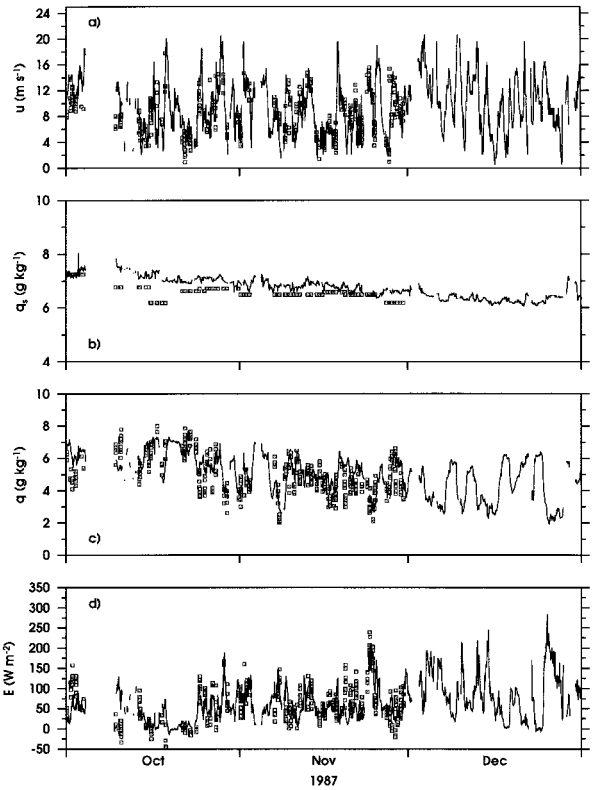

FIG. 6. As in Fig. 5 but for the period October 1987 to December 1987.

b. Local temporal variability

A good way to check the performance of the single-parameter retrievals and the combined method is a comparison to in situ time series in different geographic regions. We have chosen a 1-yr (August 1987–August 1988) time series at the weathership M and two shorter time series during the last lag of the R/V *Vickers* during TOGA COARE and the CEPEX field campaign. Figures 5, 6, 7, and 8 show the time series of latent heat flux E, near-surface humidity q, saturation humidity at the sea surface q_S, and surface wind speed u at weathership M. Again, all satellite data within 50-km distance and a time window of 1 h are included in the comparison. The gap during December 1987 and the beginning of January 1988 is caused by missing SSM/I data. The SSM/I-derived parameters q and u represents their in situ counterparts very well. For u, there is a negligible bias of 0.2 m s^{-1} and a standard deviation of 2.0 m s^{-1}, which are almost the same values as in the global comparison. The comparison for q at the weathership M shows a much better performance of the algorithm than the global comparison does. The bias is nearly zero, and the standard deviation is only 0.97 g kg^{-1}.

An obvious underestimation of the retrieved saturation humidity at the sea surface temperature is recognizable during July, August, and October 1987, as well as during the first 3 months in 1988. North of 60°N, it is expected that there are very few measurements and that the day/night observation ratio is biased toward night, due to extensive periods of cloud cover and darkness. Thus, the sea surface temperature measurement could have a temporal shift of several days or even 1 or 2 weeks. Reynolds (1993) demonstrated that the observation ratio could be biased toward night by the presence of aerosols and clouds. They found largest biases due to stratospheric aerosols from the April 1982 volcanic eruptions of El Chichón during the 1982–89 period of record. The cloud detection during nighttime is more difficult than during daytime since a combination of tests using the three infrared channels of the AVHRR instead of simple reflectance tests is required.

In spite of all these problems with the MCSST, the quality of the time series of latent heat flux is not strongly affected by the errors in the sea surface temperature, because the errors in q_S are not amplified by large errors in the retrieved wind speed. All satellite derived fluxes lie within the natural variability of the ship measurements and the variability of E at the weathership M is well represented during the one year time series. Nevertheless, the result for the sea surface temperature could

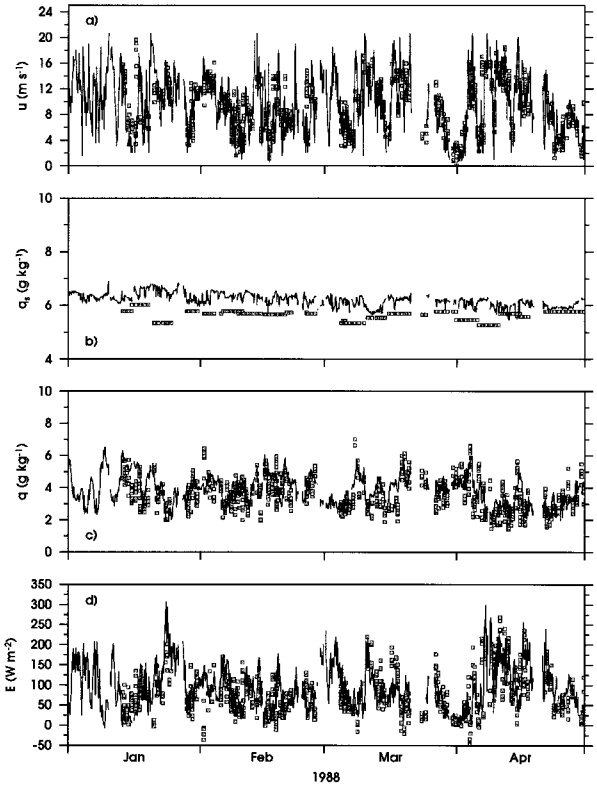

FIG. 7. As in Fig. 5 but for the period January 1988 to April 1988.

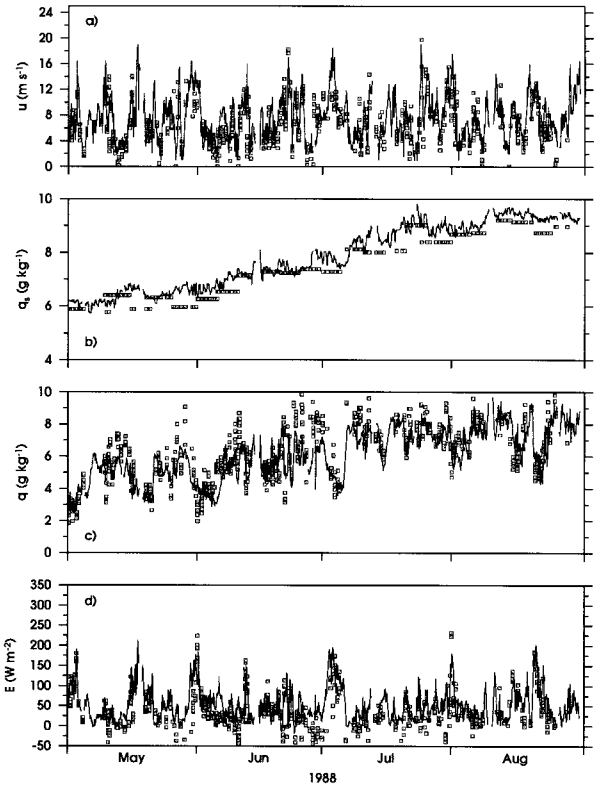

FIG. 8. As in Fig. 5 but for the period May 1988 to August 1988.

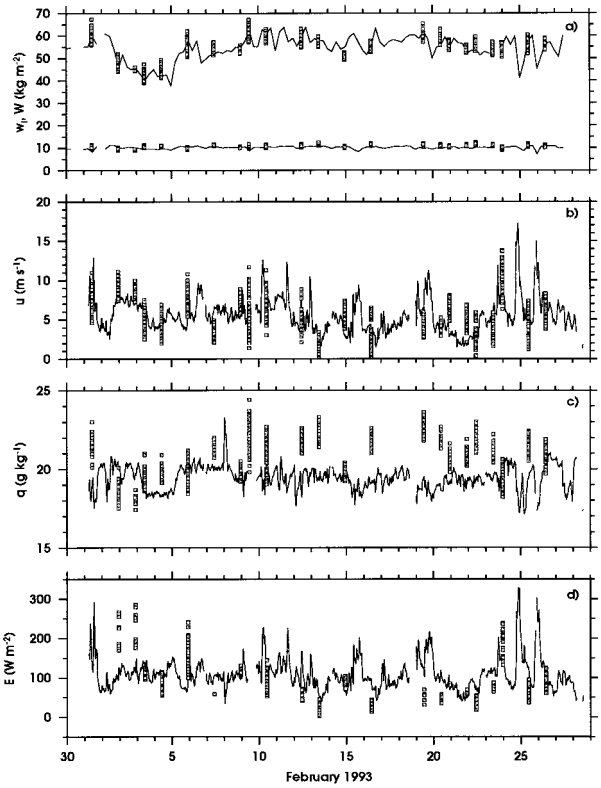

FIG. 9. Time series of (a) precipitable water of the total and 500-m bottom layer, (b) surface wind speed, (c) near-surface humidity, and (d) latent heat flux during the last phase of TOGA COARE. In situ quantities are represented by solid lines, and satellite-derived quantities by gray squares.

be improved by using bias corrected satellite data like that from Reynolds and Smith (1994).

Figures 9 and 10 show the time series of E, q, u, total precipitable water W, and w_l for TOGA COARE and CEPEX. The specific humidity of the sea surface is not shown since the ship bulk sea surface temperature has been used within the combined method, as mentioned in section 2b. The comparison criteria are the same as for the weathership M. It can be clearly seen (Figs. 9a and 10a) that precipitable water of the total and the 500-m bottom layer, as well as the surface wind speed (Figs. 9b and 10b), is retrieved excellently by the SSM/I during both experiment phases. The bottom-layer precipitable water is during the whole phase at a constant level of about 10 kg m^{-2}, and the total precipitable water shows also little variability during TOGA COARE. In spite of the good performance of the precipitable water retrievals, the directly retrieved near-surface humidity fails during the period of 10 to 25 February. This must be connected with the vertical distribution of the water vapor. At all times when the q retrieval fails, the radiosonde ascents started on the *Vickers* show very moist air above 600 hPa, with relative humidities greater than 90%, as shown in Fig. 11. This ''additional'' water vapor

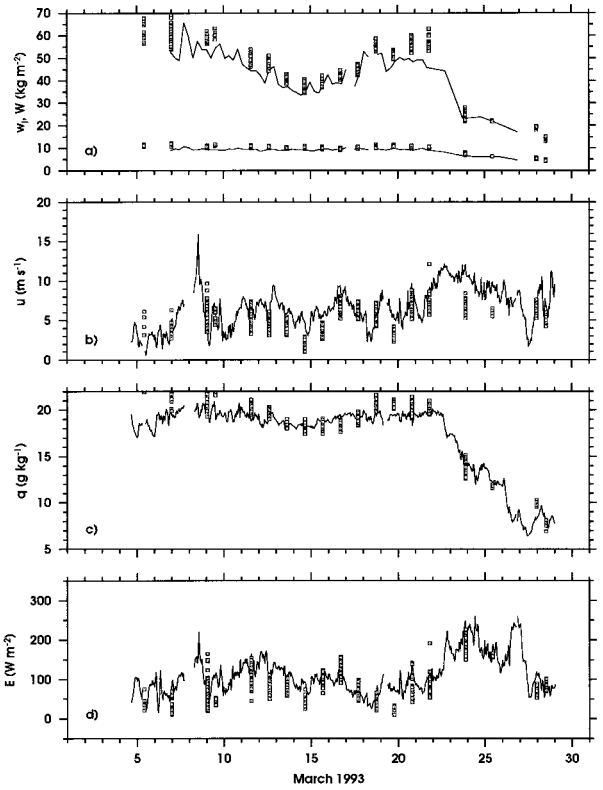

FIG. 10. As in Fig. 9 but for the CEPEX campaign.

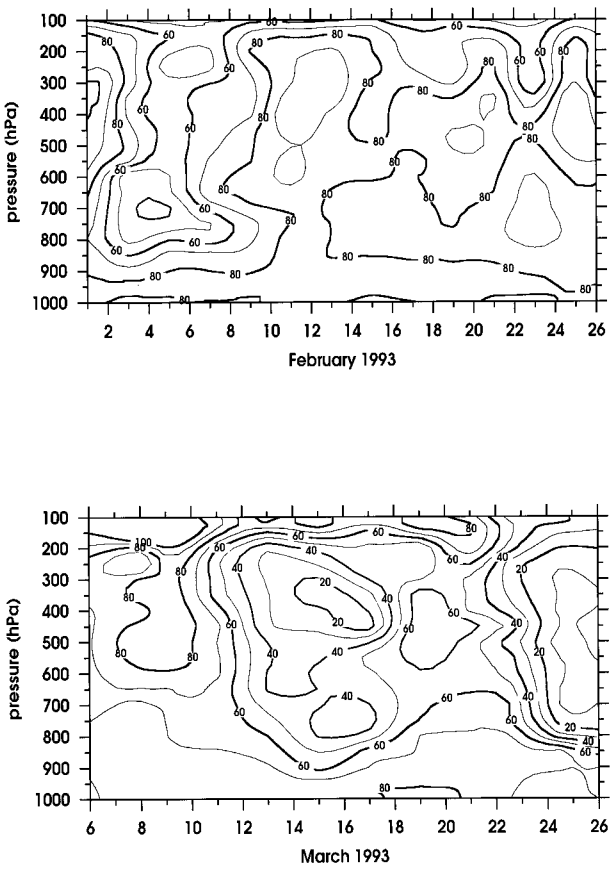

FIG. 11. Relative humidity during TOGA COARE (top panel) and CEPEX (lower panel) derived from radiosonde ascents aboard R/V *Vickers*. The contour interval is 10%, with heavy contours every 20%.

might cause a signal saturation that leads to the failure in the direct q retrieval (5).

During the first days of February and most of the CEPEX phase, the relative humidity reaches only values up to 40% above 600 hPa, and for those cases, the q retrieval works very well. The overestimation of q during February results in a systematic underestimation of the latent heat flux during this period. An attempt to use Eqs. (3) and (4) to determine q improves the result only slightly since the linear relation between q and w_l seemed not to be valid in the western tropical Pacific. An analysis of the R/V *Vickers* radiosonde data reveals that the correlation between q and w_l is only 0.39 during the phase in February. During the rest of both campaigns, we find a correlation of 0.62 that is also substantially lower than that for extratropical atmospheres, where the correlation in most of the cases is greater than 0.95 (Schulz et al. 1993). However, the representation of E is nevertheless in the range of the in situ measurements. During the last days of the CEPEX cruise, the decrease of surface humidity from tropical to extratropical regions is well represented.

c. Monthly average of latent heat flux

To show of what quality satellite-derived monthly averages $\langle E \rangle$ are, monthly averages for August and September 1987 were computed and compared to in situ measurements. As an example, Fig. 12 shows the resulting global distribution of monthly mean latent heat fluxes for September 1987. The relation of $\langle E \rangle$ to the ocean's currents is strongly pronounced since short-lived atmospheric variations are smoothed out in monthly mean fields. In the midlatitudes of the Northern Hemisphere, weak positive fluxes in the range of 50–100 W m^{-2} are recognizable. High fluxes are visible in the trade wind regions that are larger on the wintry Southern Hemisphere due to higher wind speeds. Along the ITCZ, the wind speed is lower and, therefore, the fluxes are lower too. Maximum values of $\langle E \rangle$ occur in the Indian Ocean mainly south of the equator, establishing the humidity source for the Indian summer monsoon. The moisture is transported by the Somali jet toward the Indian subcontinent.

To get an idea of the quality of remotely sensed monthly mean latent heat flux fields, the results for August and September 1987 are compared to monthly averages $\langle E \rangle$ from shipboard measurements. Such a comparison is only possible with a reduced resolution since ship measurements are widely scattered over the oceans. Hence, the monthly mean $\langle E \rangle$ based on ship measurements is computed on a $2° \times 2°$ grid in latitude and

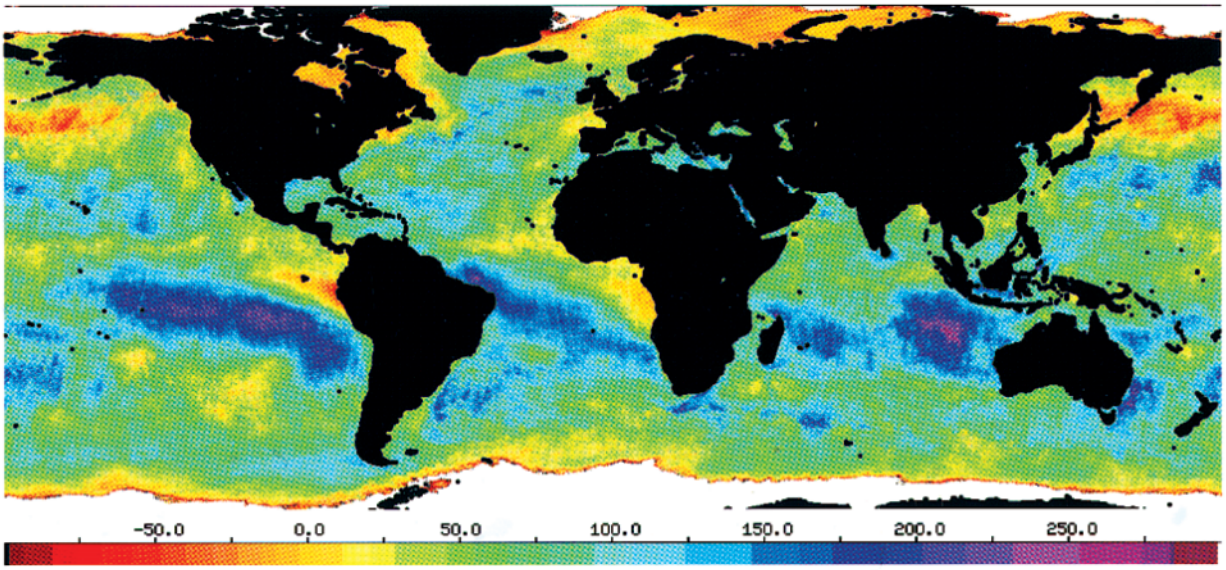

FIG. 12. Global distribution of monthly mean latent heat flux in W m^{-2} for September 1987.

longitude, and the satellite-derived latent heat flux is interpolated to this grid. The number of ship measurements per bin that is necessary to determine the monthly mean depends on the temporal and spatial variability of $\langle E \rangle$. This is equivalent to a dependence on location and season. Taylor (1984) pointed out that at least 20 measurements in a grid with 5° × 5° bins are necessary. The reduction of the bin size does not result in a decreasing number of needed observations per bin and month, since the spatial variability is decreased, but the temporal variability is increased. However, to assure that the ship observations really represent the monthly average in a 2° × 2° bin, we use only those bins with at least 25 observation days per month. The total number of observations per bin and month then ranges from 25 to 291. The resulting distribution of the 136 suitable bins is shown in Fig. 13. It can be clearly seen that the comparisons are located near the coastlines of Europe, the United States, and eastern Asia, with a few bins over the North Atlantic Ocean and the North Pacific Ocean.

A scatterplot of the monthly mean fluxes is shown in Fig. 14. Systematic differences are negligible, and a much smaller standard deviation of 20 W m^{-2} compared to instantaneous measurements is achieved. Again, this standard deviation represents both ship-derived and satellite-derived flux errors. To estimate the standard error of satellite-derived $\langle E \rangle$, we define a function $D = \langle E_{\mathrm{SSM/I}} \rangle - \langle E_{\mathrm{in\ situ}} \rangle$, which represents the difference between $\langle E \rangle$ derived from satellite data and $\langle \mathrm{E} \rangle$ derived from ship data. The error of D is D itself, since the correct value of D is zero. If we introduce this function into the standard formulation of error propagation

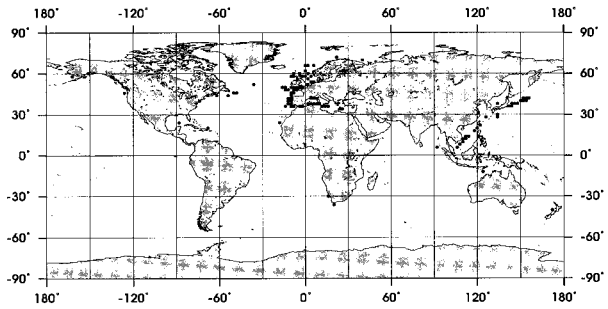

FIG. 13. Distribution of 2° × 2° grid boxes, which contain in situ measurements on at least 25 days month $^{-1}$.

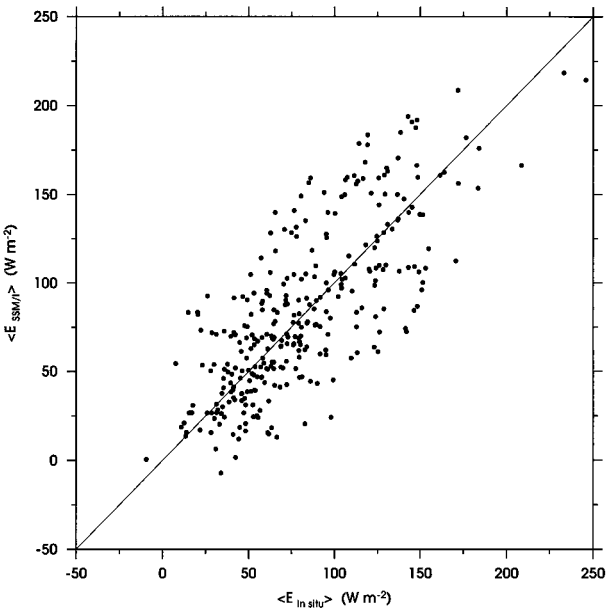

FIG. 14. Comparison between monthly mean latent heat fluxes derived from satellite data and monthly mean $\langle E_{\mathrm{in\ situ}} \rangle$ in 2° × 2° grid boxes.

$$D^2 = \left(\sigma_{\langle E_{\mathrm{SSM/I}}\rangle}\frac{\partial D}{\partial\langle E_{\mathrm{SSM/I}}\rangle}\right)^2 + \left(\sigma_{\langle E_{\mathrm{in\ situ}}\rangle}\frac{\partial D}{\partial\langle E_{\mathrm{in\ situ}}\rangle}\right)^2, \quad (8)$$

we see that we need a quantitatively estimation of the random error in the ship-derived $\langle E\rangle$ due to the ''noise'' in the ship data. To find this estimate, coincident averages of $\langle E_{\mathrm{in\ situ}}\rangle$ were compared. All single E estimates in each of the 136 bins used are divided randomly in two groups and averaged by month. The standard deviation between these coincident $\langle E\rangle$ estimates is 11 W m^{-2}. If we use this value for $\sigma_{\langle E_{\mathrm{in\ situ}}\rangle}$ in (8), then the standard deviation for $\langle E_{\mathrm{SSM/I}}\rangle$ in August and September 1987 derived from satellite data can be estimated to be approximately 15 W m^{-2}. This error estimate fits very well in the upper- and lower-bound error estimation of Chou et al. (1995) and is slightly higher than that stated by Schlüssel et al. (1995). The larger error could be caused by the fact that most of the bins used are located in coastal areas, where q, which contributes most to the error in $\langle E\rangle$, is very sensitive to land and ocean contrast (Liu et al. 1992). However, compared to earlier attempts to derive $\langle E\rangle$ from satellite data, this is a significant improvement. Esbensen et al. (1993) used the method of Liu (1986, 1988) to determine $\langle E\rangle$ and compared the result to fields estimated from the Comprehensive Ocean–Atmosphere Data Set. The evaporation fields were qualitatively similar, but the quantitative differences were large since the SSM/I estimates imply physically unrealistic downward fluxes in the mid- and high-latitude North Pacific and North Atlantic Oceans during August 1987.

6. Conclusions

Remote sensing of the latent heat flux at the air–sea interface requires combined information from different spectral regions, which is equivalent to the use of different radiometers. The required accuracy for the single-parameter retrievals is very high since the error propagation in the bulk formula leads to large errors in the derived latent heat flux.

For estimations of the sea surface temperature, the MCSST algorithm is used. In cloud-free areas, this algorithm determines the sea surface temperature with an accuracy of 0.5–1.0 K. The near-surface wind speed is retrieved from measurements of the SSM/I, and the accuracy of 1.4 m s^{-1} is confirmed by comparisons with in situ measurements. It is clearly shown that the use of the retrieved boundary layer water vapor content leads to a consistent improvement in the derivation of near-surface humidity. The boundary layer water vapor content can be retrieved from SSM/I measurements with an accuracy of 0.06 g cm^{-2}. The resulting error in the specific air humidity caused by error propagation and errors due to the regression between w_l and q is then 1.2 g kg^{-1}. If the method provided by Schlüssel et al. (1995), which is also based on the precipitable water of the 500-m bottom layer, is used, the systematic errors in the range $6 \le q \le 12$ vanish, whereas the random error is only slightly decreased to 1.1 g kg^{-1}.

The combination of the best parameter retrievals via the bulk formula allows an estimation of latent heat fluxes at the air–sea interface without any averaging if all parameters are measured at the same time and location. It is difficult to derive the absolute accuracy for the combined method since there exist only a few accurate in situ measurements of the latent heat flux. A comparison with data from merchant ships reveals a standard error of approximately 30 W m^{-2} after the deduction of errors caused by time and location differences, as well as ship errors. The comparisons of time series in the North Atlantic and in the tropical Pacific have shown that the local variability can be very well represented by the satellite measurements. Problems in the determination of the near-surface humidity arise in the western tropical Pacific when a moist layer above 600 hPa exists. This gives a reason to think about a modified retrieval scheme for q that could be deduced with the help of the vast amount of radiosoundings taken during the whole TOGA COARE campaign. The standard error of monthly mean fluxes is estimated to be 15 W m^{-2}. During the summer of 1987, the method used improves upon the method of Liu (1986, 1988) in accuracy mainly in the mid- and high latitudes.

Future improvements could be expected from a new generation of instruments to be in space in the near future. The measurement of all parameters needed in the parameterization of the latent heat flux from the same platform [AVHRR and SSM/I on the Tropical Rainfall Measuring Mission, the Moderate Resolution Imaging Spectrometer and the Multifrequency Imaging Microwave Radiometer (MIMR) on Earth Observing System-PM] reduces the problems of interpolation of data in space and time. The utilization of measurements at 1.6 μm could give the opportunity for the correction of remotely sensed sea surface temperatures with respect to atmospheric aerosol particles. The use of the MIMR has the advantage that measurements of sea surface temperatures under cloudy situations are possible too. Additionally, the retrieved precipitable water can be used for corrections of the infrared measurements of sea surface temperature.

Acknowledgments. We are grateful to William J. Emery for making available the calibrated SSM/I data and to the Data Support Section, Scientific Computing Division at NCAR for providing the in situ data. We also acknowledge the financial support of the Deutsche Forschungsgemeinschaft, the Bundesministerium für Bildung und Forschung, and the Global 3D Water Vapour Climatology Program of the Commission of the European Community. Last, we thank the two reviewers for their editorial help. All graphs have been plotted with free software supplied by Wessel and Smith (1991).

REFERENCES

Barton, I. J., A. M. Zavody, M. D. O'Brian, D. R. Cutten, R. W. Saunders, and D. T. Llewellyn-Jones, 1989: Theoretical algorithms for satellite-derived sea surface temperatures. *J. Geophys. Res.,* **94,** 3365–3375.

Blanc, T. V., 1987: Accuracy of bulk-method-determined flux, stability, and sea surface roughness. *J. Geophys. Res.,* **92,** 3867–3876.

Bunker, A. F., B. Haurwitz, J. S. Malkus, and H. Stommel, 1949: Vertical distribution of temperature and humidity over the Caribbean Sea. *Pap. Phys. Oceanogr. Meteor.,* **11,** 1–82.

Chou, S.-H., R. M. Atlas, C.-L. Shie, and J. Ardizzone, 1995: Estimates of surface humidity and latent heat fluxes over oceans from SSM/I data. *Mon. Wea. Rev.,* **123,** 2405–2425.

Crewell, S., E. Ruprecht, and C. Simmer, 1991: Latent heat flux over the North Atlantic Ocean—A case study. *J. Appl. Meteor.,* **30,** 1627–1635.

Dirks, R., R. Grossman, A. Heymsfield, J. Küttner, V. Ramanathan, and F. Valero, 1992: Central Equatorial Pacific Experiment (CEPEX). Experiment Design Center for Clouds, Chemistry and Climate, Scripps Institution of Oceanography, San Diego, CA, 54 pp.

Esbenson, S. K., D. B. Chelton, D. Vickers, and J. Sun, 1993: An analysis of errors in special sensor microwave imager evaporation estimates over the global oceans. *J. Geophys. Res.,* **98,** 7081–7101.

Eymard, L., R. Klapisz, and R. Bernard, 1989: Comparison between *Nimbus-7* SMMR and ECMWF model analysis: The problem of the surface latent heat flux. *J. Atmos. Oceanic Technol.,* **6,** 866–881.

Fairall, C., E. F. Bradley, J. S. Godfrey, G. A. Wick, J. B. Edson, and G. S. Young, 1996a. Cool skin and the warm-layer effects on sea surface temperature. *J. Geophys. Res.,* **101,** 1295–1308.

——, ——, D. P. Rogers, J. B. Edson, and G. S. Young, 1996b: Bulk parameterization of air–sea fluxes for Tropical Ocean Global Atmosphere Coupled–Ocean Atmosphere Response Experiment. *J. Geophys. Res.,* **101,** 3747–3764.

Goodberlet, M. A., C. T. Swift, and J. C. Wilkerson, 1989: Remote sensing of ocean surface winds with the Special Sensor Microwave/Imager. *J. Geophys. Res.,* **94,** 14 547–14 555.

Hollinger, J. P., R. Lo, G. Poe, R. Savage, and J. Peirce, 1987: Special Sensor Microwave/Imager user's guide. Naval Research Laboratory, Washington, DC, 177 pp.

Isemer, H. J., and L. Hasse, 1987: *Air–Sea Interaction.* Vol. 2, *The Bunker Climate Atlas of the North Atlantic Ocean,* Springer-Verlag, 252 pp.

Jacobs, C. A., 1980: Mean diurnal and shorter period variations in the air–sea fluxes and related parameters during GATE. *Deep-Sea Res.,* **26** (Suppl. I), 65–98.

Lauritson, L., G. Nelson, and F. W. Porto, 1979: Data extraction and calibration of TIROS-N/NOAA radiometers. NOAA Tech. Memo. NESS 107, 81 pp.

Liu, W. T., 1986: Statistical relation between monthly mean precipitable water and surface-level humidity over global oceans. *Mon. Wea. Rev.,* **114,** 1591–1602.

——, 1988: Moisture and latent heat-flux varibilities in the tropical Pacific derived from satellite data. *J. Geophys. Res.,* **93,** 6749–6760.

——, 1990: Remote sensing of surface turbulence heat flux. *Surface Waves and Fluxes,* G. L. Geernaert and W. J. Plant, Eds., Kluwer Academic Publishers, 293–309.

——, and P. P. Niiler, 1984: Determination of monthly mean humidity in the atmospheric surface layer over ocean from satellite data. *J. Phys. Oceanogr.,* **14,** 1452–1457.

——, K. B. Katsaros, and J. A. Businger, 1979: Bulk parameterization of air–sea exchanges of heat and water vapor including the molecular constraints at the interface. *J. Atmos. Sci.,* **36,** 1722–1735.

——, W. Tang, and F. J. Wentz, 1992: Precipitable water and surface humidity over global oceans from Special Sensor Microwave Imager and European Center for Medium Weather Forecasts. *J. Geophys. Res.,* **97,** 2251–2264.

Llewellyn-Jones, D. T., P. J. Minnett, R. W. Saunders, and A. M. Zavody, 1984: Satellite multichannel infrared measurements of sea surface temperature of the NE Atlantic Ocean using AVHRR/2. *Quart. J. Roy. Meteor. Soc.,* **110,** 613–631.

Luthardt, H., 1985: Estimation of mesoscale surface fields of meteorological parameters in the North Sea area from routine measurements. *Beitr. Phys. Atmos.,* **58,** 255–272.

Marchuk, G., V. Kondratyev, and V. Kozoderov, 1990: The heat balance components. *Earth Radiation Budget: Key Aspects,* Nauka Publishers, 204–211.

McClain, E. P., 1981: Multiple atmospheric-window techniques for satellite-derived sea surface temperatures. *Oceanography from Space,* J. Gower, Ed., Plenum, 73–85.

——, W. G. Pichel, and C. C. Walton, 1985: Comparative performance of AVHRR-based multichannel sea surface temperatures. *J. Geophys. Res.,* **90,** 11 587–11 601.

McMillin, L. M., and D. S. Crosby, 1984: Theory and validation of the multiple window measurements with different absorption. *J. Geophys. Res.,* **89,** 5113–5117.

Monaldo, F. M., 1988: Expected differences between buoy and radar altimeter estimates of wind speed and significant wave height and their implications on buoy-altimeter comparisons. *J. Geophys. Res.,* **93,** 2285–2302.

Reynolds, R. W., 1993: Impact of Mount Pinatubo aerosols on satellite-derived sea surface temperatures. *J. Climate,* **6,** 768–774.

——, and T. M. Smith, 1994: Improved global sea surface temperature analyses. *J. Climate,* **7,** 929–948.

Schlüssel, P., 1989: Satellite-derived low-level atmospheric water-vapour content from synergy of AVHRR with HIRS. *Int. J. Remote Sens.,* **10,** 705–721.

——, 1995: Passive Fernerkundung der unteren Atmosphäre und der Meeresoberfläche aus dem Weltraum. Berichte aus dem Zentrum für Meeres- und Klimaforschung, Reihe A: Meteorologie 20, 175pp. [Available from Universität Hamburg Meteorologisches Institut, Bundesstraße 55, D-20146 Hamburg, Germany.]

——, and H. Luthardt, 1991: Surface wind speeds over the North Sea from Special Sensor Microwave/Imager observations. *J. Geophys. Res.,* **96,** 4845–4853.

——, H.-Y. Shin, W. J. Emery, and H. Grassl, 1987: Comparison of satellite-derived sea surface temperatures with in situ skin measurements. *J. Geophys. Res.,* **92,** 2859–2874.

——, L. Schanz, and G. Englisch, 1995: Retrieval of latent heat flux and longwave irradiance at the sea surface from SSM/I and AVHRR measurements. *Adv. Space Res.,* **16,** 107–116.

Schulz, J., 1993: Fernerkundung des latenten Wärmeflusses an der Meeresoberfläche. Ph.D. dissertation, Universität Hamburg, 108 pp.

——, P. Schlüssel, and H. Graßl, 1993: Water vapour in the atmospheric boundary layer over oceans from SSM/I measurements. *Int. J. Remote Sens.,* **14,** 2773–2789.

Simonot, J. Y., and C. Gautier, 1989: Satellite estimations of surface evaporation in the Indian Ocean during the 1979 monsoon. *Ocean–Air Int.,* **1,** 239–256.

Smith, S. D., 1988: Coefficients for sea surface wind stress, heat flux, and wind profiles as a function of wind speed and temperature. *J. Geophys. Res.,* **93,** 2859–2874.

Taylor, P. K., 1982: Remote sensing of atmospheric water content and sea surface latent heat flux. *Proc. Annual Technical Conf. on Remote Sensing and the Atmosphere,* Reading, United Kingdom, Remote Sensing Society, 265–272.

——, 1984: The determination of surface fluxes of heat and water by satellite microwave radiometry and in situ measurements. *Large-Scale Oceanographic Experiments and Satellites,* C. Gautier and M. Fieux, Eds., D. Reidel, 223–246.

Walton, C. C., 1988: Nonlinear multichannel algorithms for estimating sea surface temperature with AVHRR satellite data. *J. Appl. Meteor.*, **27,** 115–124.

WCRP 1990: Scientific Plan for the TOGA Coupled Ocean–Atmosphere Response Experiment. WCRP Publ. Series 3 Addendum, WMO/TD-64 Addendum, 90 pp. [Available from TOGA COARE International Project Office, University Corporation for Atmospheric Research, P.O. Box 3000, Boulder, CO 80307-3000.]

Wells, N. C., and S. King-Hele, 1990: Parameterization of tropical ocean heat flux. *Quart. J. Roy. Meteor. Soc.*, **116,** 1213–1224.

Wentz, F. J., 1989: User's manual SSM/I geophysical tapes. Tech. Rep. 060989, 16 pp.

——, 1992: Measurement of oceanic wind vector using satellite microwave radiometers. *IEEE Trans. Geosci. Remote Sens.*, **30,** 960–972.

——, L. A. Mattox, and S. Peteherych, 1986: New algorithms for microwave measurements of ocean winds: Applications to SEASAT and the Special Sensor Microwave/Imager. *J. Geophys. Res.*, **91,** 2289–2307.

Wessel, P., and W. H. F. Smith, 1991: Free software helps map and display data. *Eos, Trans. Amer. Geophys. Union*, **72,** 445–446.

Wick, G. A., W. J. Emery, and P. Schlüssel, 1992: A comprehensive comparison between satellite-measured skin and multichannel sea surface temperature. *J. Geophys. Res.*, **97,** 5569–5595.

Wilheit, T. T., Jr., J. R. Greaves, J. A. Gatlin, D. Han, B. M. Krupp, A. S. Milman, and E. S. Chang, 1984: Retrieval of ocean surface parameters from the Scanning Multifrequency Microwave Radiometer (SMMR) on the *Nimbus-7* satellite. *IEEE Trans. Geosci. Remote Sens.*, **22,** 133–143.